ELSEVIER

Journal of Quantitative Spectroscopy & Radiative Transfer 89 (2004) 257–269

Journal of Quantitative Spectroscopy & Radiative Transfer

www.elsevier.com/locate/jqsrt

Simulation of rainbows, coronas and glories using Mie theory and the Debye series

Philip Laven

Geneva, Switzerland

Received 31 December 2003; received in revised form 4 April 2004

Abstract

The scattering of light from homogeneous spheres might be considered to be a trivial problem because rigorous solutions, such as Mie theory, were developed almost 100 years ago. Nevertheless, full-colour simulations of atmospheric optical effects, such as rainbows, coronas and glories, reveal several intriguing issues. Calculations using the Debye series can help us to understand the scattering mechanisms causing specific effects: for example, the atmospheric glory seems to be caused by light rays that have suffered one internal reflection within water drops.

Keywords: Atmospheric optics; Rainbow; Corona; Glory; Mie theory; Debye series

1. Introduction

Rigorous solutions for scattering of light from homogeneous spheres (e.g. Mie theory [1]) were developed almost 100 years ago. For many years, the computational complexity of Mie theory limited its practical application, but modern personal computers can now be used to produce full-colour simulations of atmospheric optical effects, such as rainbows, coronas and glories. This paper is based on graphs and simulations generated by the MiePlot computer programme [2] freely available from the author at http://www.philiplaven.com/mieplot.htm.

Fig. 1 shows Mie theory calculations of intensity as a function of scattering angle θ for monochromatic red light ($\lambda = 0.65$ μm) for spherical water drops of different radius r. Mie theory

E-mail address: philip@philiplaven.com (P. Laven).

0022-4073/$ - see front matter
doi:10.1016/j.jqsrt.2004.05.026

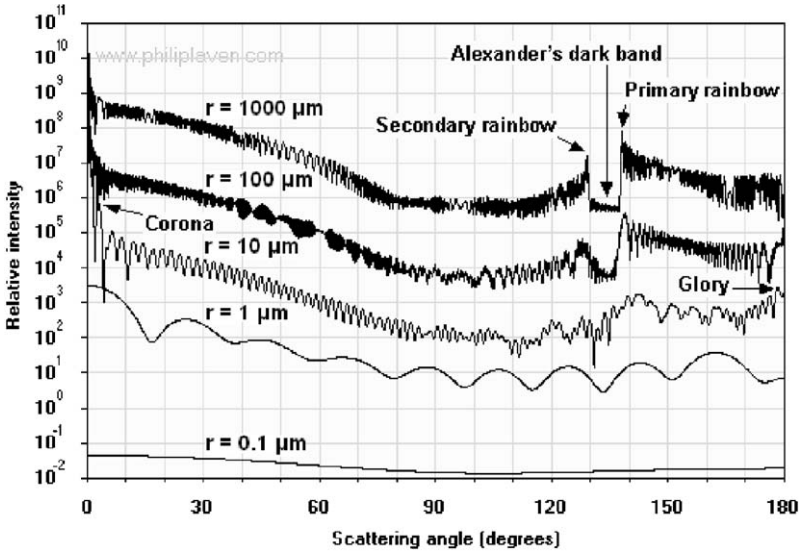

Fig. 1. Mie theory calculations showing scattering of monochromatic light of wavelength 0.65 μm from spherical water drops with radius $r = 0.1–1000$ μm.

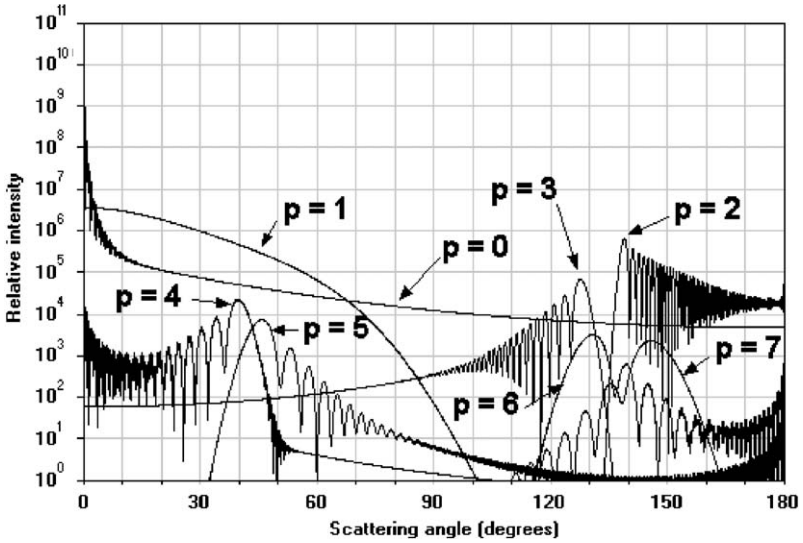

Fig. 2. Debye series calculations showing scattering of monochromatic light of wavelength 0.65 μm from a spherical water drop with radius $r = 100$ μm.

is rigorous, but it provides no indication of the scattering mechanisms causing particular features. As shown in Fig. 2 for scattering of red light by a water drop with $r = 100$ μm, the Debye series [3–5] can separate the contributions made by light rays of order p, where $p = 0$ corresponds to external reflection and diffraction; $p = 1$ corresponds to direct transmission through the sphere; $p = 2$ corresponds to 1 internal reflection; $p = 3$ corresponds to two internal reflections—and so on. For $p \geqslant 1$, the number of internal reflections is given by $(p - 1)$.

As is well known from geometric optics, Fig. 2 confirms that the primary rainbow is caused by $p = 2$ rays and that the secondary rainbow is caused by $p = 3$ rays. It should be noted that the Debye series calculations are rigorous: Mie theory gives the same result as the vector sum of Debye series calculations for all integer values of $p \geqslant 0$.

2. Rainbows

Fig. 3 shows Mie theory simulations of various rainbows caused by the scattering of sunlight by spherical water drops of radius r between 10 and 500 μm. For very small water droplets (e.g. for $r = 10$ μm), the rainbow (or fogbow) is almost white and not clearly defined. For $r = 50$ μm, the

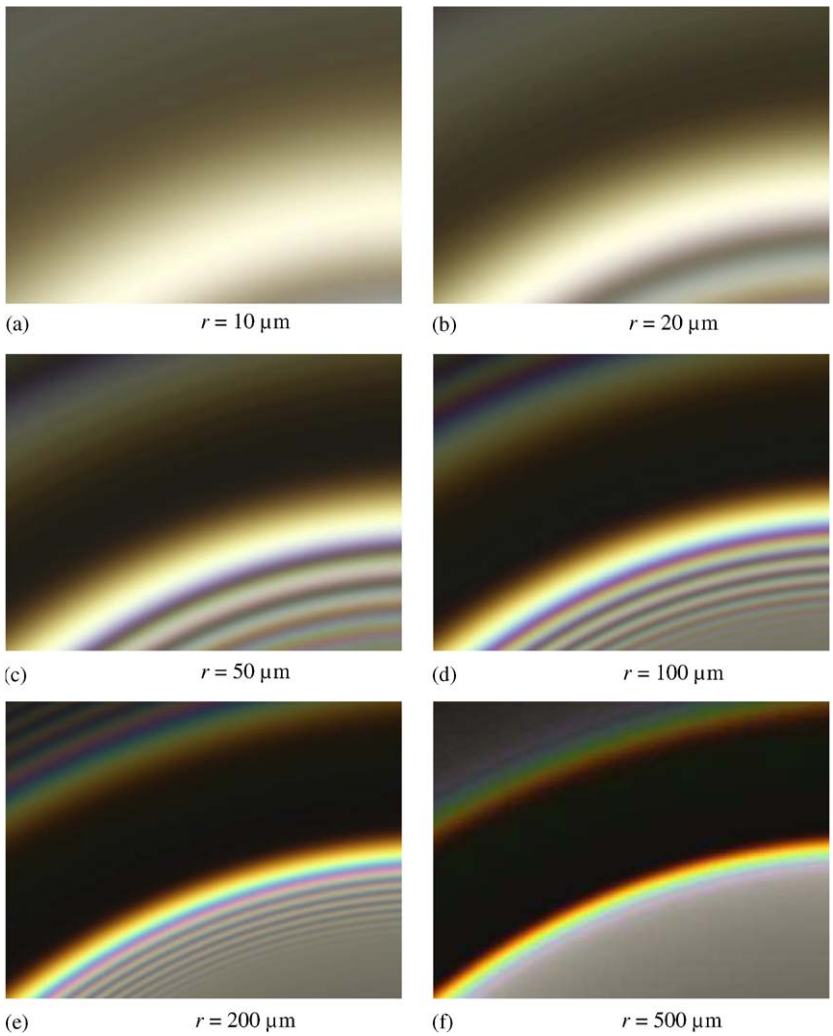

Fig. 3. (a–f) Simulations of primary and secondary rainbows caused by scattering of sunlight from spherical water drops of specified radius r (as would be seen by a 35 mm camera with a lens of 70 mm focal length).

primary rainbow is predominantly white with a hint of red at its outer edge. The colours of the primary rainbow become more obvious for larger drops, together with the fainter secondary rainbow and Alexander's dark band. Supernumerary arcs can be clearly seen inside the primary rainbow for $r = 50$, 100 and 200 μm, as well as on the outside of the secondary rainbow for $r = 100$ and 200 μm. However, the supernumerary arcs disappear for larger water drops because the angular separation between such arcs is less than the sun's apparent angular diameter of 0.5°.

Fig. 4 shows a graph of intensity calculated using Mie theory for scattering of sunlight from a water drop with $r = 100$ μm showing the primary and secondary rainbows. The three horizontal bars above the graph show the colours of the primary and secondary rainbows for perpendicular polarisation, parallel polarisation and for unpolarised light: note that both rainbows are strongly polarised—as indicated by the very dark bar corresponding to parallel polarisation. Fig. 5 shows an equivalent graph identifying the separate contributions due to the Debye $p = 0, 2, 3$ and 6 terms. Comparison of Figs. 4 and 5 indicates that, as expected, the primary and secondary rainbows are caused by $p = 2$ and 3 rays, respectively, while the darkness of Alexander's dark band is determined by the $p = 0$ term (in this case, the $p = 0$ term is due to reflection from the exterior of the drop). Note that all of these calculations ignore the effects of multiple scattering: Gedzelman and Lock [6,7] have taken account of multiple scattering in their studies of glories, cloudbows and coronas using Mie theory.

Lee [8] introduced a powerful technique to illustrate how the appearance of rainbows varies with drop size. Fig. 6 shows three examples of these "Lee diagrams" in which each coloured point represents the colour of light scattered in a specific direction by a drop of radius r—in this case for values of r between 10 and 1000 μm. The brightness of each vertical line of colours representing the primary rainbow caused by a drop of radius r has been normalised by the maximum

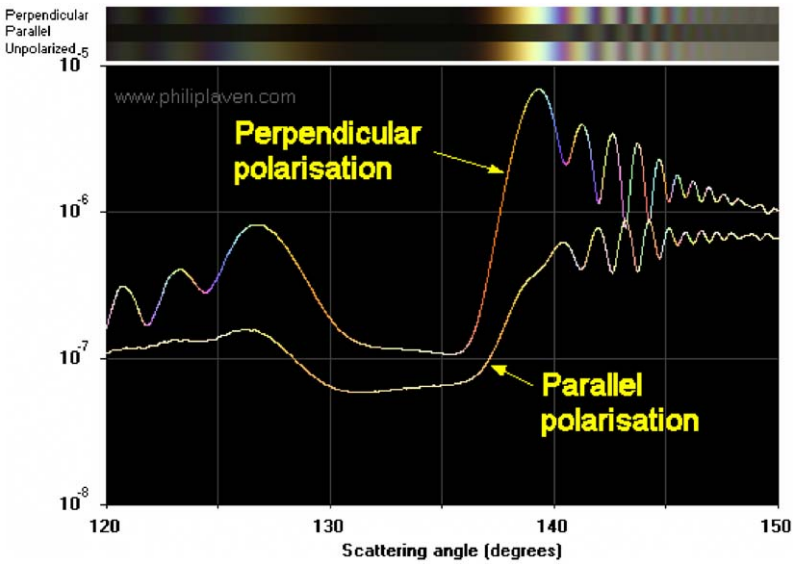

Fig. 4. Mie theory calculations showing the primary and secondary rainbows caused by scattering of sunlight from a spherical water drop with radius $r = 100$ μm.

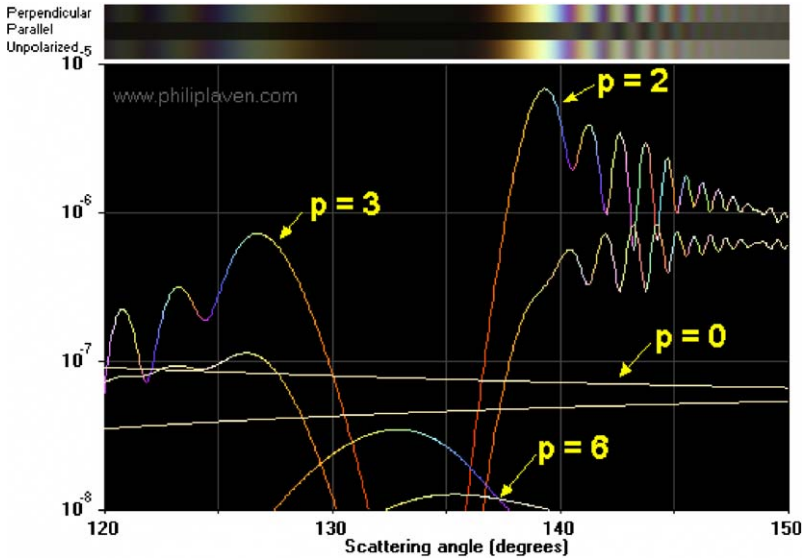

Fig. 5. Debye series calculations showing the primary and secondary rainbows caused by scattering of sunlight from a spherical water drop with radius $r = 100$ μm.

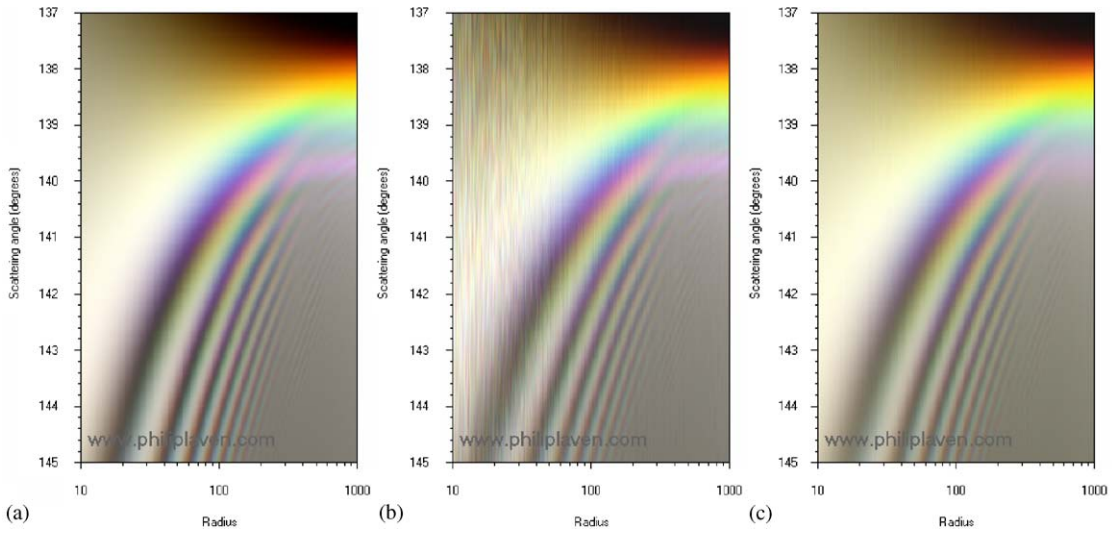

Fig. 6. Lee diagrams showing the primary rainbow caused by the scattering of sunlight by spherical water drops as a function of radius $r = 10 - 1000$ μm: (a) Airy theory (7 wavelengths); (b) Mie theory (7 wavelengths) and (c) Mie theory (30–600 wavelengths).

luminance for that value of r. Fig. 6a is based on Airy theory, whereas Figs. 6b and c are based on Mie theory. Figs. 6a and b show the results of representing the continuous spectrum of sunlight by seven discrete wavelengths spaced equally between 380 and 700 nm, whereas Fig. 6c is based on a

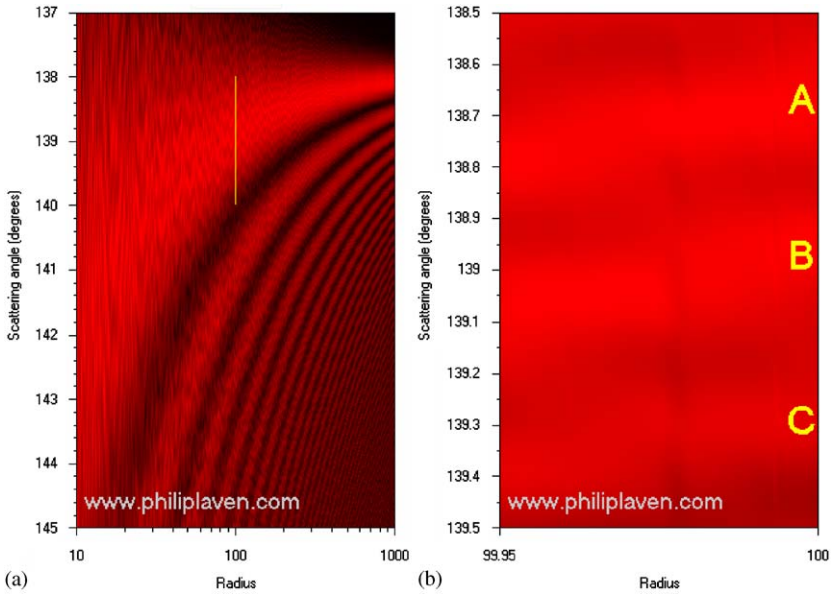

Fig. 7. Lee diagrams for scattering of monochromatic light ($\lambda = 0.65$ μm) from spherical water drops: (a) Scattering angles between 137° and 145° for radius $r = 10$–1000 μm and (b) Expanded portion of Fig. 7a (indicated by yellow line in Fig. 7a).

much larger number (ranging from 600 wavelengths for $r = 10$ μm to 30 wavelengths for $r > 200$ μm).

Note that Figs. 6a and c are very similar, whereas Fig. 6b is affected by "unnatural marbling" as noted by Lee. This marbling disappears if the sun's spectrum is represented by a very large number of discrete wavelengths as in Fig. 6c—but what happens if the number of wavelengths is reduced to one? Fig. 7a shows that the marbling becomes even more prominent for monochromatic light ($\lambda = 0.65$ μm). Fig. 7b, which shows an enlarged portion of Fig. 7a, indicates that the marbling is actually a set of diagonal stripes of varying brightness. As marked by the letters A, B and C, the stripes in Fig. 7b correspond to the maxima of the high-frequency ripples shown in Fig. 8.

Although Mie theory was used to generate Fig. 8, the complicated pattern of ripples can be explained by using geometric optics. The diagram in Fig. 9 shows three separate rays that result in a scattering angle $\theta = 141°$: rays 1 and 2 undergo one internal reflection in the sphere ($p = 2$), while ray 3 is reflected from the exterior of the sphere ($p = 0$). As the amplitudes of rays 1 and 2 are similar, constructive interference occurs when the optical path difference between rays 1 and 2 is $n\lambda$ (where n is an integer), whereas the rays almost cancel each other when the optical path difference between them is $(n + 0.5)\lambda$. As the path difference between rays of types 1 and 2 depends on the scattering angle, the scattered intensity varies with scattering angle θ— as shown in Fig. 10, where the vector sum of the $p = 2$ contributions is plotted as the "Debye $p = 2$" curve, corresponding to the supernumerary arcs of the primary rainbow. The vector sum of the $p = 0$ and 2 contributions is shown in Fig. 10 as the "Debye $p = 2$ and 0" curve, which agrees fairly closely with the curve calculated using Mie theory—thus confirming that $p = 0$ rays cause the

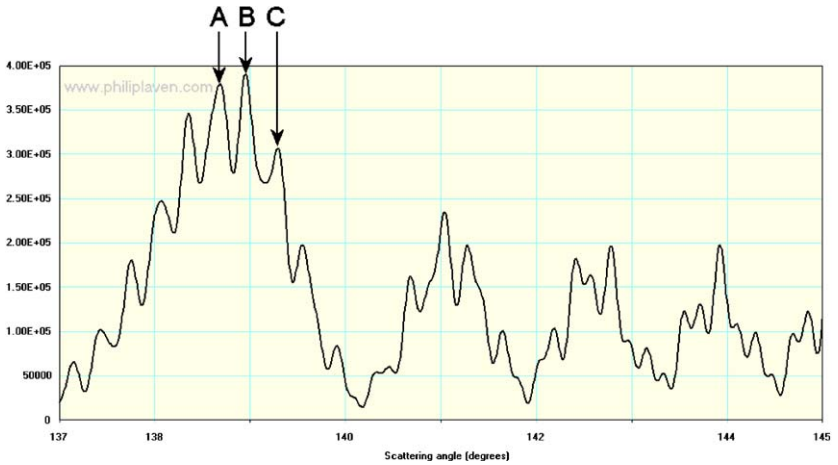

Fig. 8. Mie theory calculations showing the primary rainbow caused by scattering of monochromatic red light ($\lambda = 0.65$ μm) from a spherical water drop with $r = 100$ μm (The ripples marked A, B and C correspond to the brighter stripes marked A, B and C in Fig. 7b).

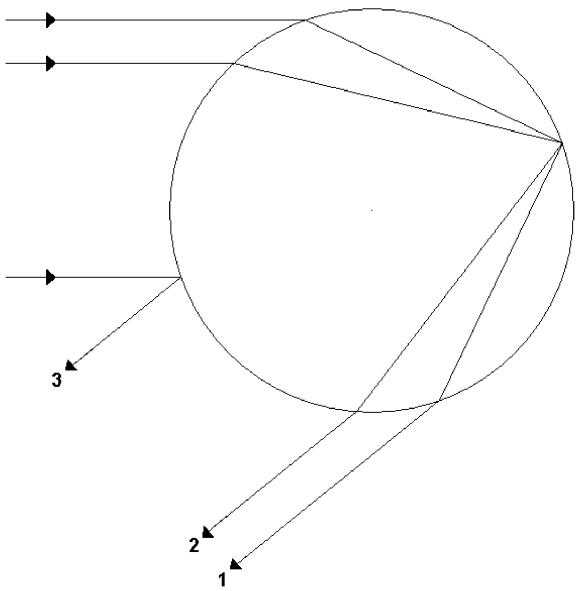

Fig. 9. Geometric ray tracing shows that, for a refractive index of 1.33257, two Debye $p = 2$ rays (1 and 2) and one Debye $p = 0$ ray (3) produce a scattering angle of 141°.

high-frequency ripples superimposed on the $p = 2$ curve. As the relative phases of the $p = 0$ and 2 rays change very rapidly as a function of r and θ, a complicated pattern of diagonal lines appears on Lee diagrams.

Mie theory is in itself rigorous, but Lee diagrams such as Fig. 6b indicate that simulations using Mie theory can give unreliable results—for example, where a continuous spectrum is

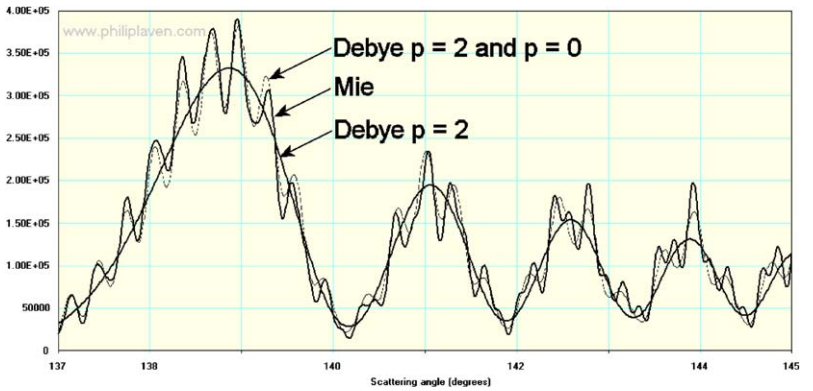

Fig. 10. Calculations using Mie theory and the Debye series showing the primary rainbow caused by scattering of monochromatic red light ($\lambda = 0.65$ μm) from a spherical water drop with $r = 100$ μm. *N.B. The differences between "Mie" and "Debye $p = 2$ and $p = 0$" curves can be explained by minor contributions from Debye $p = 3$, $p = 6$ and $p = 7$ rays.*

approximated by a few discrete wavelengths. Such problems can be avoided by using a very large number of wavelengths, but this dramatically increases the computational effort. In some respects, using Mie theory to simulate rainbows is like using "a sledge-hammer to crack a nut"—especially as the much simpler Airy theory gives similar results with much less effort.

3. Coronas

The corona often appears as a series of concentric coloured rings around a cloud-covered moon. This phenomenon is widely attributed to diffraction around small droplets of water in the clouds, but Lock and Yang [9] highlighted significant differences between the diffraction model and Mie theory for simulations of the corona.

The Lee diagrams in Fig. 11 compare the diffraction model with Mie theory for scattering of sunlight from water droplets with r between 0.1 and 10 μm. Fig. 11a shows the results of diffraction calculations. As the brightest scattering occurs at $\theta = 0^\circ$, Fig. 11a contains little information because the corona is very much darker than the forward scattered light—and computer displays cannot reproduce the necessary large dynamic range. To overcome this problem, the brightness of Fig. 11b has been increased by a factor of 10 so that the top part of it is "over-exposed", but the colours of the corona become visible. The data from Fig. 11a have been re-plotted in Fig. 11c so as to remove the brightness information, instead showing the saturated colour of each pixel. This shows that, according to the diffraction model, the sequence of colours in the corona is independent of r. As the outer rings tend towards white, Fig. 11c suggests that no more than two rings of the corona will be visible even under optimum viewing conditions. Although diagrams based on saturated colours (such as Fig. 11c) are useful for comparing colours, it must be emphasised that they do not represent the appearance of scattered light.

Looking now at the equivalent diagrams (Figs. 11d–f) produced using Mie theory, the key difference between Figs. 11a and d is that, for r between 0.5 and 2 μm, Mie theory predicts

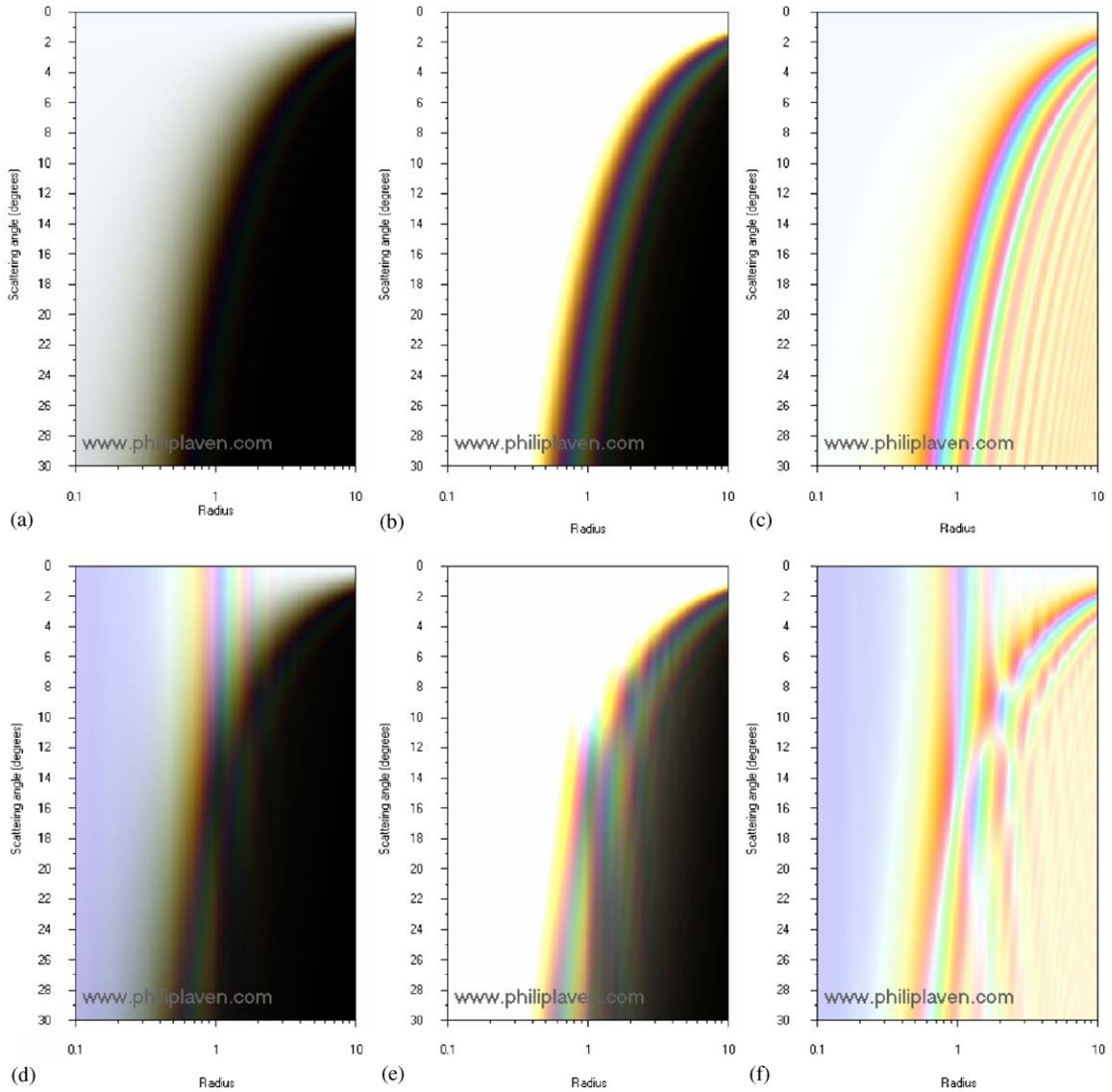

Fig. 11. Lee diagrams showing the corona caused by the scattering of sunlight by spherical water drops as a function of radius $r = 0.1 - 1000$ μm: (a) diffraction, (b) diffraction (brightness × 10), (c) diffraction (saturated colours), (d) Mie theory, (e) Mie theory (brightness × 10) and (f) Mie theory (saturated colours).

uniform bands of colour at scattering angles θ of less than about 8°: for example, red for $r = 0.8$ and 1.6 μm and violet for $r = 1$ μm. Comparison of Figs. 11b and e shows that Mie theory produces very complex patterns for $r < 3$ μm. Comparison of Figs. 11c and f indicates that Mie theory and diffraction calculations produce similar results for $r > 5$ μm, but the diffraction model is totally inadequate for $r < 3$ μm. Fig. 11f also confirms the findings of Gedzelman and Lock [7]

who reported that "*The sequence of corona colours changes rapidly for small droplets but becomes fixed once droplet radius exceeds about* 6 μm".

An enlarged portion of Fig. 11f is shown in Fig. 12, where there seem to be "islands" of fairly uniform colour. The boundaries between many of these islands are often white lines—which merge with other white lines at various points in the diagram. What causes these complicated patterns of colours? The Debye series can help us to understand the scattering mechanisms: Fig. 13 indicates that the Mie theory curve for $r = 2$ μm is essentially the sum of the Debye $p = 0$ and 1 terms—corresponding to diffraction around the sphere and transmission through the sphere, respectively. The Mie curve for $r = 2$ μm is essentially identical to the Debye $p = 0$ term when θ is less than about 7°, whilst the Debye $p = 1$ term is dominant when θ is greater than about 15°. Between these two zones, the $p = 0$ and 1 terms are of comparable intensity: the resulting interference between these two scattering mechanisms is the main reason for the complicated patterns of colours shown in Fig. 12. However, it is not clear what causes the uniform bands of colour at low values of θ as depicted in Fig. 11d—nor, indeed, whether they correspond to any optical effects observed in the atmosphere.

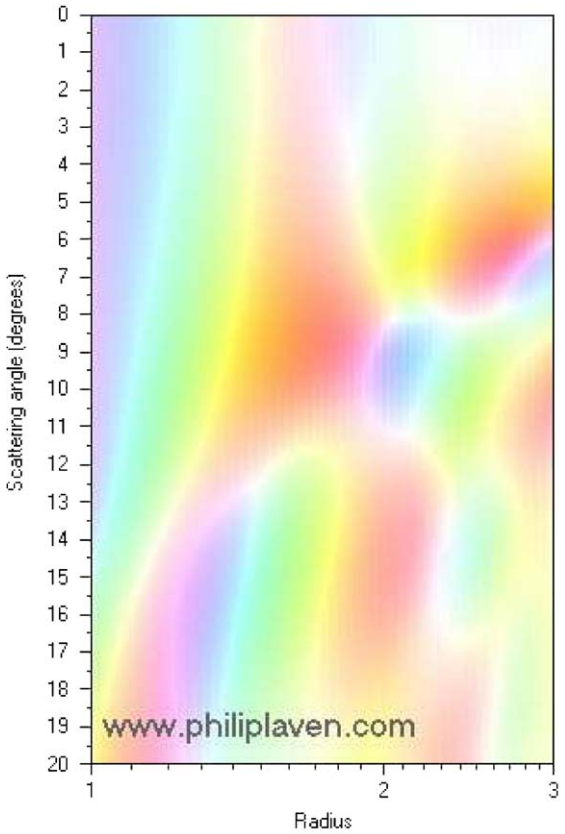

Fig. 12. Enlarged portion of Fig. 11f showing saturated colours for radius $r = 1 - 3$ μm.

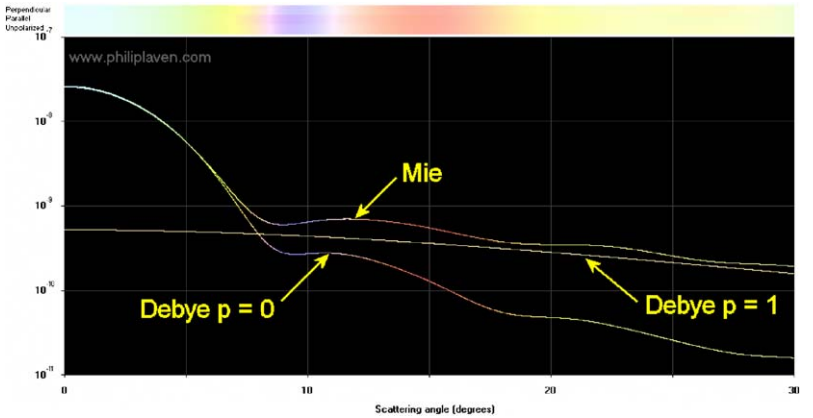

Fig. 13. Calculations using Mie theory and the Debye series showing the corona caused by scattering of sunlight from a spherical water drop with radius $r = 2$ μm. *Note that the coloured bars above the graph show saturated colours, as in Fig. 12.*

4. Glories

In the past, sightings of glories were rare and usually associated with the Brocken Spectre, in which a mountaineer's shadow on fog or clouds is surrounded by a series of concentric coloured rings. Nowadays, glories are seen much more frequently surrounding the shadow of an aircraft on clouds: the author has taken about 1000 pictures of glories while travelling on commercial aircraft within the last 3 years.

Glories are usually explained by lots of scientific "arm waving"—for example, Bohren and Huffmann [10] state: *"Unlike the rainbow, the glory is not easy to explain, other than to say that it is a consequence of all of the thousands of terms in the scattering series, a correct but unsatisfying statement."* Following the pioneering work in 1947 of van de Hulst [11], the modern consensus is that glories are caused by a combination of surface waves and rays that have undergone many internal reflections.

Mie theory can be used to simulate glories, but it does not offer any explanation for their formation. Fig. 14 shows curves of intensity calculated using Mie theory and the Debye series for scattering of sunlight from a spherical drop of water with $r = 10$ μm. Fig. 14 shows that the Debye $p = 2$ term (i.e. corresponding to light that has suffered one internal reflection in the sphere) is dominant in forming the glory, but substantial contributions in the vicinity of 180° are also made by $p = 11$, 7, 6 and higher order terms. In practice, terms other than $p = 2$ contribute very little to intensity of the scattered light for $\theta < 179°$. However, with the exception of the $p = 0$ curve (which is effectively white), the other curves show almost identical colours as a function of θ—such as the red colours around 177.7° and 176.2°. It seems unlikely that this is a coincidence.

Fig. 15 shows two simulations of the glory caused by scattering of sunlight from a spherical drop of water with $r = 10$ μm: the left-hand side shows a simulation based only on the Debye $p = 2$ contribution, while the right-hand side is based on Mie theory. The key difference is that, as indicated in Fig. 14, Mie theory predicts a bright white zone at the centre (i.e. θ approaching 180°). More importantly, both simulations produce essentially identical sequences of coloured

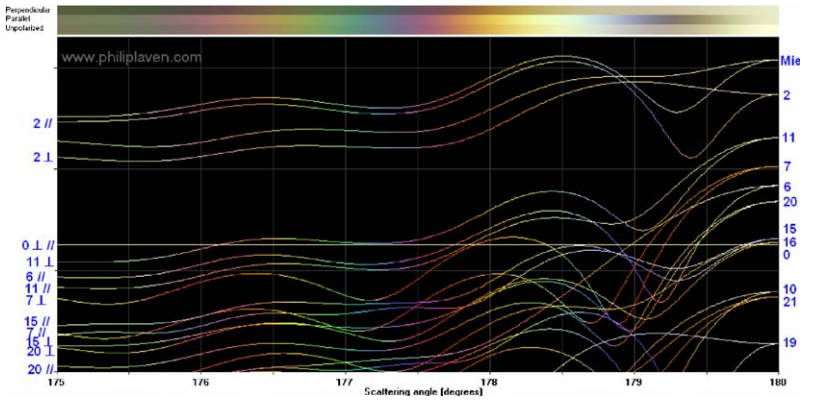

Fig. 14. Comparison of Mie theory and Debye series calculations for scattering of sunlight from a spherical water drop with radius $r = 10\,\mu\text{m}$ ($n//$ and $n_\perp$ denote $p = n$ for parallel and perpendicular polarisation, respectively).

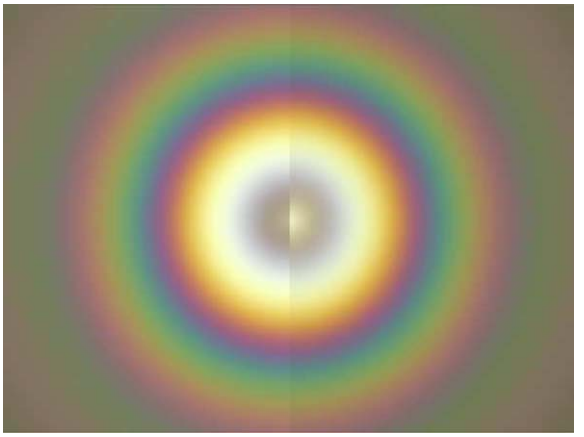

Fig. 15. Simulations of a glory caused by scattering of sunlight from a spherical water drop with radius $r = 10\,\mu\text{m}$: comparison of Debye series $p = 2$ (left) and Mie theory (right) calculations. As the width of this image corresponds to an angle of about $\pm 5^\circ$, it shows scattering angles between 175° and 180°.

rings, thus confirming that the coloured rings of the atmospheric glory are primarily caused by light that has suffered only one reflection within the water drop.

5. Conclusions

Although scattering of light from homogeneous spherical particles may seem to be a trivial problem, simulations of atmospheric optical effects using Mie theory indicate several unresolved issues. Diagrams mapping the scattered intensity as a function of radius r and scattering angle θ are valuable aids to understanding scattering phenomena—especially when they highlight

departures from the expected patterns. Calculations using the Debye series can help us to understand the scattering of light by spherical particles: for example, the coloured rings of glories seem to be caused by light that has been reflected once within water drops (i.e. the Debye $p = 2$ term), while the bright white central feature is mainly due to higher-order terms.

References

[1] Mie G. Beitrage zur Optik trüber Medien, speziell kolloidaler Metallosungen. Ann Phys Leipzig 1908;25:377–445.
[2] Laven P. Simulation of rainbows, coronas, and glories by use of Mie theory. Appl Opt 2003;42:436–44.
[3] Debye P. Das elektromagnetische feld um einen zylinder und die theorie des Regenbogens. Phys Z 1908;9(22):775–8.
[4] Hovenac E, Lock JA. Assessing the contributions of surface waves and complex rays to far-field Mie scattering by use of the Debye series. J Opt Soc Am A 1992;9(5):781–95.
[5] Grandy WT. Scattering of waves from large spheres. Cambridge, UK: Cambridge University; 2001.
[6] Gedzelman SD. Simulating glories and cloudbows in color. Appl Opt 2003;42:429–35.
[7] Gedzelman SD, Lock JA. Simulating coronas in color. Appl Opt 2003;42:497–504.
[8] Lee Jr. RL. Mie theory, airy theory, and the natural rainbow. Appl Opt 1998;37:1506–19.
[9] Lock JA, Yang L. Mie theory model of the corona. Appl Opt 1991;30:3408–14.
[10] C.F. Bohren, D.R. Huffman. Absorption and scattering of light by small particles. New York: Wiley; 1983, p. 389.
[11] van de Hulst HC. A theory of the anti-coronae. J Opt Soc Am 1947;37:16–22.